

# Modeling of Laser Processing for Advanced Silicon Solar Cells

G. Poulain<sup>\*1</sup>, D. Blanc<sup>1</sup>, A. Kaminski<sup>1</sup>, B. Semmache<sup>2</sup> and M. Lemit<sup>1</sup>

<sup>1</sup>Université de Lyon; Institut des Nanotechnologies de Lyon INL-UMR5270, CNRS, INSA de Lyon, Villeurbanne, F-69621, France

<sup>2</sup>SEMCO Eng., 625, rue de la Croix Verte - Parc Euromédecine, 34196 Montpellier Cedex 5 - France

\*Corresponding author: gilles.poulain@insa-lyon.fr

**Abstract:** Silicon solar cells still require cost reduction and improved efficiency to become more competitive. New architectures can provide a significant increase in efficiency, but today most of the approaches need additional processing steps. In this context, laser processing offers a unique way to replace technological steps like photolithography that is not compatible with the requirements of the photovoltaic industry.

This paper discusses some aspects of the simulation of these new laser processes. Selective ablation of dielectric with a nanosecond UV laser is studied to remove locally antireflection and passivation coatings at the front surface of silicon solar cells in order to take electric contacts. At the same time the influence of induced localized thermal effects on phosphorous-doped silicon emitters is investigated. Modeling results are compared to experimental data, especially SIMS measurements of the phosphorous doping profile.

**Keywords:** laser processing, dielectric ablation, dopant diffusion, silicon solar cells

## 1. Introduction

Selective laser ablation of dielectric is a promising way to remove locally antireflection and passivation coatings (silicon nitride) at the front surface of silicon solar cells in order to take electric contacts with self-aligned electrochemical metal contact deposition [1].

Thermal effects associated with ablation have an impact on the cell emitter (phosphorus-doped region at silicon surface). It is important to understand how the doping profile evolved with the incident laser energy. It is indeed essential to maintain a high concentration of dopant at the surface to ensure good electrical contact.

In this work, we discuss the modeling of laser ablation of a silicon nitride layer (SiN) and the doping profile evolution with COMSOL Multiphysics. Laser-matter interaction of one

laser pulse (UV, nanosecond) is studied. Surface texturation of the cell is not taken into account in this model.

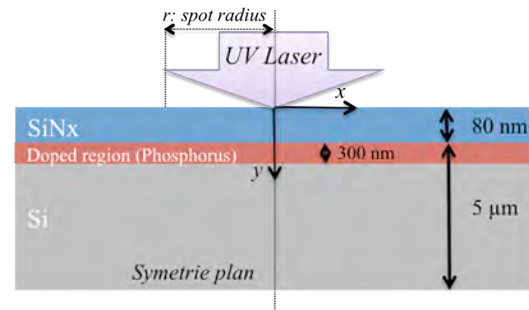


**Figure 1:** Sample structure and geometry

Results are compared with experimental measurements of the ablated area and with secondary ion mass spectroscopy (SIMS) measurements of the phosphorous doping profile.

## 2. Governing equations

The differential equation describing the thermal effects is the heat-transfer equation:

$$\rho(T)C_p(T)\frac{\partial T}{\partial t} = \nabla[k_{th}(T)\nabla T] + Q \quad (1)$$

Where  $\rho(T)$  is the material density,  $C_p(T)$  the specific heat capacity,  $T$  the temperature,  $t$  the time,  $k_{th}$  the thermal conductivity and  $Q$  the heat source in volume due to absorbed laser power.

The heat source term can be written as follows:

$$Q = (1 - R(T))\alpha(T)P_{in}(x,t)I(y) \quad (2)$$

Where  $\alpha(T)$  is the material absorption coefficient,  $R(T)$  the surface reflectivity,  $P_{in}$  the incident laser power and  $I(y)$  the relative intensity given by the Beer-Lambert law:

$$I(y) = \exp(-\alpha(T)|y|) \quad (3)$$

The incident laser power is distributed in time and space with a Gaussian shape. According to the notation used in Figure 1:

$$P_{in}(x,t) = P_0 \exp\left\{-\left(\frac{t-t_0}{\tau/2}\right)^2\right\} \exp\left\{-\left(\frac{x}{r}\right)^2\right\} \quad (4)$$

Where  $P_0$  is the peak power of the laser beam,  $t_0$  the time shift,  $\tau$  the pulse time,  $r$  the beam radius at half height.

The absorption coefficient  $\alpha(T)$  and the reflectivity  $R(T)$  can be calculated from the complex refractive index  $n-ik$  :

$$\alpha(T) = \frac{4\pi k(T)}{\lambda} \quad (5)$$

$$R(T) = \frac{(n(T)-1)^2 + k(T)^2}{(n(T)+1)^2 + k(T)^2} \quad (6)$$

Where  $\lambda$  is laser wavelength.

The differential equation describing the diffusion process is the Fick's second law:

$$\frac{\partial c}{\partial t} = \nabla[D(T)\nabla c] \quad (7)$$

Where  $c$  is the phosphorous concentration,  $D(T)$  the diffusion coefficient in silicon,  $T$  the temperature and  $t$  the time.

### 3. Use of COMSOL Multiphysics

#### 3.1 Thermal model

Transient conduction analysis of the “*Heat Transfer mode (2D)*” has been chosen to solve the heat conduction equation. The geometry of the sample is made of two rectangles with dimensions reported in Figure 1.

Various constants and scalar expressions are necessary to describe the laser pulse and the physical properties of both materials. They are reported in Table 1. Physical properties of the materials are temperature dependant. We used the smoothed heavyside function (*flc2hs*) implemented in COMSOL to describe the abrupt

changes with temperature. Latent fusion heat ( $E_{lm}$ ) was taken into account with an arbitrary increase of the heat capacity ( $C_{p,lm}$ ) around fusion temperature [2] defined by:

$$E_{lm} = \int C_{p,lm} dT \quad (8)$$

The heat source term of the subdomain settings is due to the absorbed laser power and is given by (2).

Boundary conditions of the left, bottom and right side (Fig. 1) are adiabatic (thermal insulation):

$$\hat{n}(k_{th} \nabla T) = 0 \quad (9)$$

Where  $\hat{n}$  is the normal vector of the surface.

Boundary conditions at the top surface have to include thermal radiation and heat transfer to ambient room:

$$\hat{n}(k_{th} \nabla T) = q_0 + h(T_{inf} - T) + \sigma \varepsilon (T_{amb}^4 - T^4) \quad (10)$$

Where  $q_0$  is the inward heat flux (equals to  $\theta$ , the incident energy is already taken into account in the term source  $Q$ ),  $h$  is the convective heat transfer coefficient,  $T_{inf}$  is the external temperature,  $\sigma$  is the Stefan-Boltzmann constant,  $\varepsilon$  is the emissivity and  $T_{amb}$  the ambient temperature.

#### 3.2 Diffusion model

Transient diffusion analysis of the “*Convection and Diffusion mode (2D)*” has been added to the previous model to describe phosphorus atom diffusion. Geometry of the model is the same as the one used previously. The initial value of the phosphorus concentration is given by experimental data and the diffusion coefficient is reported in Table 1.

#### 3.3 Meshing and solver parameters

The absorption coefficient of silicon in the UV is around  $10^8 \text{ m}^{-1}$  and the absorption length is around 10 nm. Therefore, the maximum element size at the silicon surface has to be 1 nm. To facilitate the meshing, the substrate can be divided in order to have a finer meshing under the irradiated area.

Ranges of the time parameters vary from 0 to 60 ns with a step of 1 ns (0.1 ns during the laser pulse from 10 ns to 40 ns). The linear system solver used is PARDISO.

## 4. Results and discussion

### 4.1 Laser heating and ablation

Due to the low absorption coefficient of the silicon nitride, the laser absorption in SiN is negligible and the heat source term is five orders of magnitude lower than in silicon (Figure 2). As observed in Figure 3, the heat absorbed in Si is transferred by conduction in a few nanoseconds to SiN. The Si substrate behaves therefore as a heat source after having absorbed the laser energy.

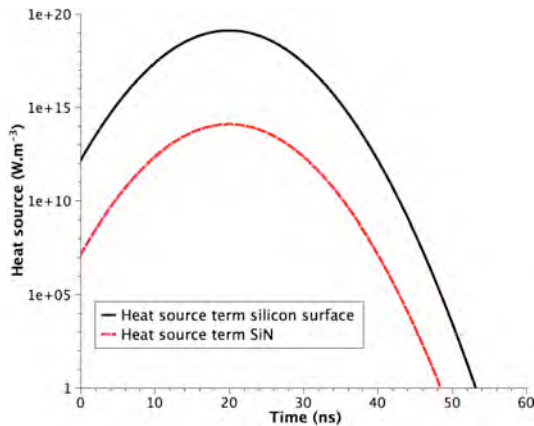


**Figure 2:** Heat source term in silicon nitride and silicon substrate. Incident laser energy of  $0.1 \text{ J.cm}^{-2}$ .

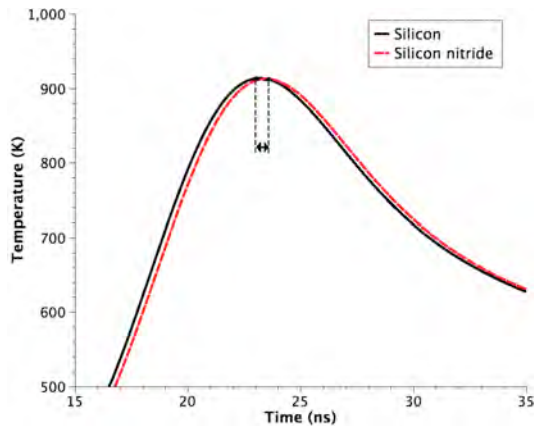


**Figure 3:** Temperature versus time for silicon nitride and silicon. Incident laser energy of  $0.1 \text{ J.cm}^{-2}$ .

The maximum temperature reached in SiN determines the ablation of the antireflection coating. The removal of the SiN occurs for a temperature around 2150 K. At this point the partial pressure of the  $\text{N}_2$  in the SiN reaches one atmosphere and this leads to the dielectric decomposition [3].

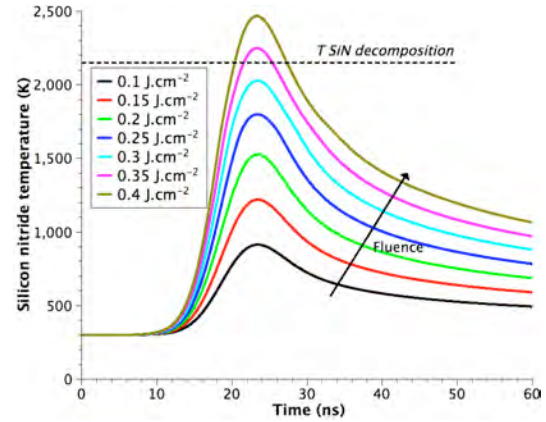


**Figure 4:** Temperature versus time in SiN for various laser fluence. Note that temperature evolution above 2150 K is not taken into account in this model.

Simulation showed that the silicon nitride removal begins at incident laser fluence about  $0.35 \text{ J.cm}^{-2}$  (Figure 4), in good agreement with the literature [4] and with our experimental data (Figure 5).

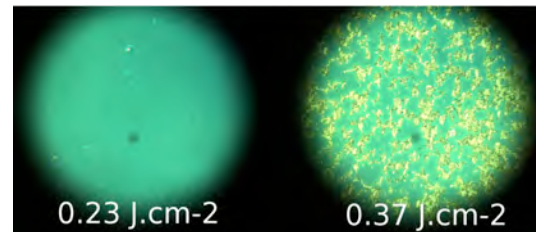


**Figure 5:** Optical microscopy pictures of SiN removal with laser. Silicon surface appears in bright yellow and silicon nitride in green.

The temperature field in SiN can give an estimation of the ablated zone by plotting the area of the SiN subdomains where  $T > 2150 \text{ K}$ . However, simulation results lead to an overestimated radius of the ablated zone compared to the measurements made using an optical microscope ( $10 \mu\text{m}$  simulated instead of  $5 \mu\text{m}$  experimental for a laser fluence of  $0.4 \text{ J.cm}^{-2}$ ).

<sup>2</sup>). This difference can be explained by the fact that the evolution of the optical properties of the sample surface above 2150 K was not taken into account in this model.

#### 4.2 Evolution of the dopant profile

Simulations were made for a 60  $\Omega$  initial emitter, corresponding to a standard phosphorus doping profile used in photovoltaics. Modeling results were compared to SIMS measurements (Fig. 6).

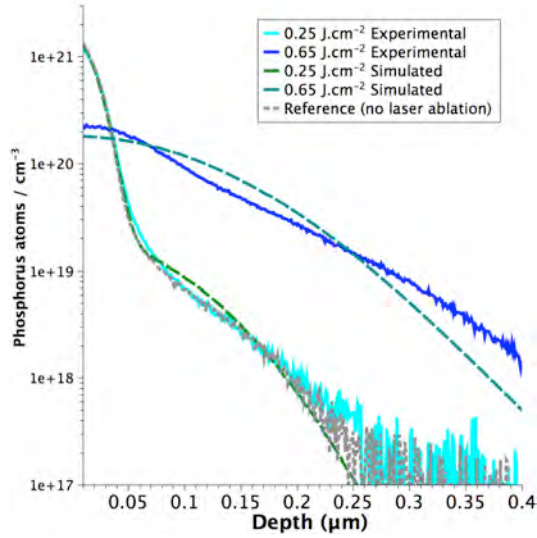


**Figure 6:** Experimental data and simulated results of phosphorus profile in silicon.

SIMS measurements were performed over a 50  $\mu\text{m}$  diameter area, therefore the simulated curves were obtained by averaging the different concentration profiles obtained at different  $x$  values underneath the laser pulse.

SIMS profiles could be reasonably well approximated with the theoretical curves at low ( $0.25 \text{ J.cm}^{-2}$ ) and high ( $0.65 \text{ J.cm}^{-2}$ ) fluence despite the drastically different diffusion profiles. Indeed at  $0.65 \text{ J.cm}^{-2}$  there is a large increase in diffusion coefficient ( $\times 10^7$ ) because silicon is melted.

In both cases the surface concentration was also calculated within a good approximation of the experimental value.

#### 5. Conclusion

Modeling results are consistent with the different experimental measurements performed. The

minimal laser fluence required to initiate the ablation of the silicon nitride layer has been evaluated. Evolution of the phosphorus profile induced by laser ablation has also been estimated.

This model can be easily adapted to simulate others laser processing used to realize advanced silicon solar cells. For example, by changing the properties of the upper layer to a doping glass, it is possible to simulate the implementation of selective emitters, which rely on high dopant concentration localised under the front electrical contacts and lightly doped areas between the front fingers. This model will be improved in future work to include the changes in optical properties of the top surface above 2150 K. Another step will be to study the influence of surface texturing with the COMSOL RF module.

#### 6. Appendix

Parameters	Value/Fonction
$F_p$ (laser fluence)	2 [ $\text{J.cm}^{-2}$ ]
$\tau$	10 [ns]
$t_0$	20 [ns]
$r$	12.5 [ $\mu\text{m}$ ]
$P_0$	$F_p * (2/\sqrt{\pi}) * \tau$ [ $\text{W.m}^{-2}$ ]
$\lambda$	355 [nm]
$\alpha_{Si}$	$10^8 \text{ [m}^{-1}\text{]}$
$\alpha_{SiN}$	$10^3 \text{ [m}^{-1}\text{]}$
$R_{SiN}$	0.45
$h$	10 [ $\text{W.m}^{-2}.\text{K}^{-1}$ ]
$T_{f,Si}$	1687 [K]
$E_{lm}$	1650 [ $\text{J.g}^{-1}$ ]
$H$	$\text{flc2hs}(T-T_{f,Si},0.1)$
$C_p$	$703+(965-703)*H+C_{plm}$ [ $\text{J.kg}^{-1}.\text{K}^{-1}$ ]
$\rho_{Si}$	$2330+(2500-2330)*H$ [ $\text{kg.m}^{-3}$ ]
$k_{rh,Si}$	$148+(200-148)*H$ [ $\text{W.m}^{-1}.\text{K}^{-1}$ ]
$D_{Phosphorus}$	$10.5 * \exp(-3.69/(8.617e-5 * T)) * (T < T_{f,Si} + 0.1) + (5e-4) * H$ [ $\text{m}^2.\text{s}^{-1}$ ]

**Table 1:** Parameters used in the simulation

#### Acknowledgments

The authors thank C. Dubois for the SIMS measurements.

This work was sponsored by the French Agency for Environment and Energy Management (ADEME).

## References

- [1] A. Knorz, M. Peters, A. Grohe, C. Harmel, R. Preu, Selective laser ablation of SiN<sub>x</sub> layers on textured surfaces for low temperature front side metallization, Prog. Photovolt: Res. Appl. 17 (2009) 127-136.
- [2] J.R. Köhler, S. Eisele, Influence of precursor layer ablation on laser doping of silicon, Progress in Photovoltaics: Research and Applications. 18 (2010) 334-339.
- [3] S.A.G.D. Correia, J. Lossen, M. Wald, K. Neckermann, M. Bähr, Selective laser ablation of dielectric layers, in: Proceedings of 22nd European Photovoltaic Solar Energy Conference, Milan, 2007.
- [4] V. Rana, Z. Zhang, C. Lazik, R. Mishra, T. Weidman, C. Eberspacher, Investigations into selective removal of silicon nitride using laser for crystalline silicon solar cells, in: Proceedings of 23rd European Photovoltaic Solar Energy Conference, Valence, 2008.